IOPscience iopscience.iop.org

Home Search Collections Journals About Contact us My IOPscience

Impact of thermal annealing on interfacial layer and electrical properties of a-SiN_x : H/Si

This article has been downloaded from IOPscience. Please scroll down to see the full text article.

2010 EPL 90 26002

(http://iopscience.iop.org/0295-5075/90/2/26002)

View the table of contents for this issue, or go to the journal homepage for more

Download details:
IP Address: 124.124.247.13
The article was downloaded on 06/06/2010 at 17:38

Please note that terms and conditions apply.

A LETTERS JOURNAL EXPLORING THE FRONTIERS OF PHYSICS

April 2010

EPL, **90** (2010) 26002 www.epljournal.org
doi: 10.1209/0295-5075/90/26002

Impact of thermal annealing on interfacial layer and electrical properties of a-SiN$_x$: H/Si

SARAB PREET SINGH[1], G. VIJAYA PRAKASH[1], S. GHOSH[1], SANJAY RAI[2] and P. SRIVASTAVA[1(a)]

[1] *Nanostech Laboratory, Department of Physics, IIT Delhi - Hauz Khas, New Delhi-110 016, India*
[2] *X-ray Optics Section, Raja Ramanna Centre for Advanced Technology - Indore 452 013, India*

received 13 November 2009; accepted in final form 7 April 2010
published online 11 May 2010

PACS 61.05.cm – X-ray reflectometry (surfaces, interfaces, films)
PACS 73.40.Qv – Metal-insulator-semiconductor structures (including semiconductor-to-insulator)
PACS 79.60.Jv – Interfaces; heterostructures; nanostructures

Abstract – We report the impact of post-deposition thermal annealing (in nitrogen ambient) on the evolution of an interfacial layer between a hydrogenated amorphous silicon nitride (a-SiN$_x$: H) thin film and a Si(100) substrate and its correlation with electrical properties. X-ray reflectivity measurements reveal that the SiN$_x$ films under different post annealing temperatures demonstrate variation in the density, thickness and roughness. Also it is found that the interface state density (D_{it}) is directly related to the interfacial layer density of the film rather than to the surface and interface roughness.

Copyright © EPLA, 2010

Silicon nitride (SiN$_x$) has been used as a gate and passivation dielectric material [1,2], especially in display devices such as organic/inorganic thin film transistors [3,4], wherein the gate dielectric and dielectric-semiconductor interfaces play a critical role in field-effect operations [5,6]. SiN$_x$ films deposition is usually done by chemical vapour deposition methods, and the films are generally found to be hydrogenated, amorphous, chemically non-stoichiometric, and thermally unstable. Moreover, the evolution of an interface layer (IL) between SiN$_x$ and the Si substrate prevails when the bonding at the interface deviates from ideal bonding, and as a consequence due to the generation of electrically active defects there is an adverse affect on the performance of the device [7–9]. Therefore, the research has been focused on structural and post annealing factors to control the growth of SiN$_x$/Si interface [10–14]. However, such interfaces are not very well understood or optimized in terms of variation in density evolution and its correlation with electrical properties. To the best of our knowledge, there are hardly any studies of SiN$_x$/Si systems, which simultaneously look at the variation of density along the thickness of films and their electrical characterization. Therefore, the focus of the present work is to investigate the structural evolution of the interfacial layer during SiN$_x$ deposition, post-annealing process and correlate its microscopic packing with electrical properties.

Hg-sensitized Photo-CVD (chemical vapour deposition) with a 253.7 nm low-pressure lamp was used to deposit a-SiN$_x$: H thin films on the n-type Si(100) substrate at 200 °C and 0.8 torr. Prior to deposition, the Si substrate was cleaned using a RCA technique. In order to obtain a change in film stoichiometry the gas flow rate was varied. The flow rate of SiH$_4$ (2% in argon) was kept at 10 and 20 sccm and that of NH$_3$ at 10 sccm. As a consequence, the ratio $R = [\mathrm{SiH_4}]/[\mathrm{NH_3}]$ turns out to be 0.02 and 0.04, respectively. As-deposited (ASD) films were thermally annealed in N$_2$ ambient at 900, 1000 and 1100 °C for 1 hour, respectively. X-ray reflectivity (XRR) measurements were performed by using Cu $K\alpha$ ($\lambda = 0.154$ nm) radiation with a home-made reflectometer [15]. For electrical measurements, aluminium (Al) was thermally evaporated and then patterned as gate electrode of MIS capacitors. C-V measurements were carried without post-metallization annealing at 1 MHz at room temperature under dark and electrically shielded conditions.

XRR is a very sensitive technique to find out thickness, roughness and density of different layers of the films [16]. Figure 1 shows the XRR experimental profiles (open red circles) along with fitted curves (solid black lines) as a function of wave vector transfer $q = 4\pi \sin\theta/\lambda$ for ASD and annealed films. It is noticeable from fig. 1 that the

(a) E-mail: pankajs@physics.iitd.ac.in

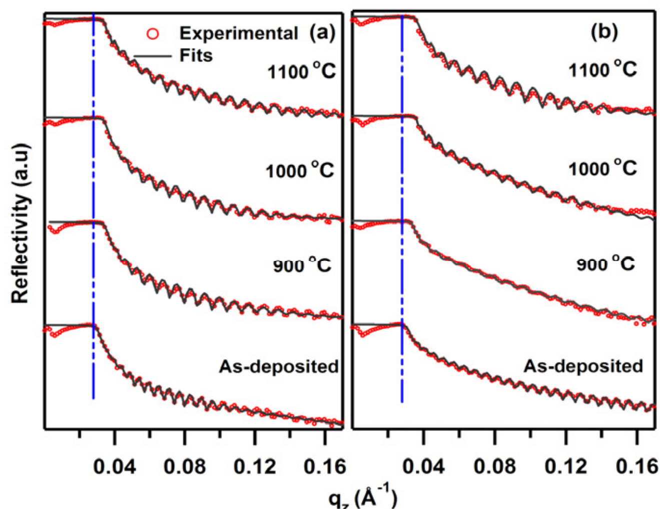

Fig. 1: (Colour on-line) X-ray reflectivity curves both experimental (open red circles) and fitted (solid black lines) as a function of wave vector transfer "q_z (Å^{-1})" for as-deposited and annealed samples (a) $R = 0.02$ and (b) $R = 0.04$, respectively. (The blue dotted line is to guide the eye for an increase in the density of the ASD films on annealing.)

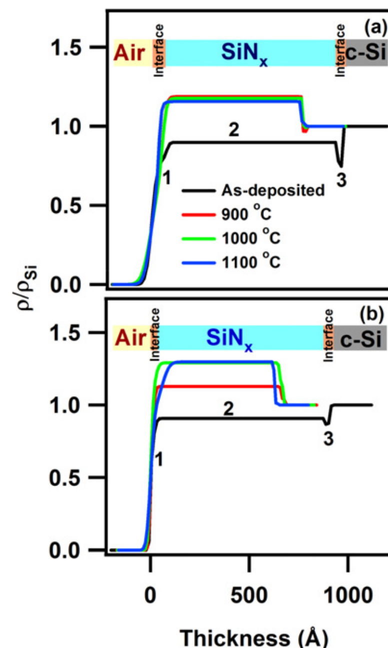

Fig. 2: (Colour on-line) The electron density profiles normalized to the Si substrate as obtained from the fit for the as-deposited and annealed samples, (a) $R = 0.02$ and (b) $R = 0.04$, respectively, along with the representative fitted model.

value of critical angle (shown by the blue dotted line to guide the eye) increases on annealing indicating increase in the density of ASD films. Simultaneously increase in oscillation width indicates reduction in film thickness. A well-known Parratt recursive formalism along with Nevot-Croce model for roughness was used to extract details of film thickness, roughness and density of different layers from the XRR data [17]. The value of roughness for the interface between the IL and Si substrate was taken as 0.4 nm in the fitting procedure. χ^2-minimization technique along with non-linear square fitting algorithm was used to refine the thickness, roughness and density values. During the refinement it became clear that it is not possible to fit the experimental data with a single layer of SiN_x on Si substrate. Thus to improve the fitting quality a systematic addition of more layers was done. The best-fit model extracted by fitting the reflectivity data suggests that all films have three-layer structures. These layers are defined as top layer, corresponding to mixture of SiO_2 (usually present due to the oxidation of the top surface of the film) and SiN_x, middle layer, corresponding to SiN_x and bottom IL, which has different density and roughness values compared to the middle layer. It should be noted that fitting of reflectivity data is not possible if we remove any of the layer from the model. The parameters that are obtained from the best fit (plotted in fig. 1) using the recursive formalism are tabulated in table 1. Uncertainty in the value of thickness, density and roughness of the films are 1%, 5% and 5%, respectively, and are mentioned with the maximum value wherever required. In addition to this, the roughness-convoluted scattering length density (SLD) of the structure as a function of thickness was calculated using the Parratt-32 software[1] [17]. First, film parameters have been determined by fitting the experimental XRR profile. Subsequently these parameters were used to calculate SLD. SLD is defined as

$$\rho_{\mathrm{SLD}}(z) = \sum\nolimits_{i=1}^{N} \frac{\rho_i - \rho_{i+1}}{2} \left(1 + \operatorname{erf}\left(\frac{z - z_i}{\sqrt{2}\sigma_i}\right)\right),$$

where, N is the total number of layers, $\rho_i = \frac{2\pi\delta}{\lambda^2}$ is the scattering length density of the i-th layer at position (z_i) and with a Gaussian roughness (σ_i), the error function is approximated by a fifth-order polynomial. SLD was further divided by the value of Thomson scattering length ($r_0 \sim 2.8 \times 10^{-5}$) to get the respective electron density profile (EDP) *i.e.*

$$\rho_{\mathrm{SLD}}(z) = \text{Electron density}\,[\rho(z)] \times r_0.$$

In general, the following can be observed by the values listed in table 1 and the electron density profiles (EDP) of the samples normalized to Si substrate, ρ/ρ_{Si} as shown in fig. 2. Both sets of ASD and annealed samples ($R = 0.02$ and $R = 0.04$) have three-layer structure. In all the samples IL has the lowest roughness. The roughness of the top layer is larger than that of the middle layer for $R = 0.02$ samples, while it is the contrary for $R = 0.04$ samples. The density profile is not uniform throughout the thickness of the film. It is minimal at the film/Si interface, it increases and saturates in the middle followed by a gradual decrease at the top in all cases due to oxidation.

[1]Parratt-32, Version 1.5.

Table 1: Parameters obtained from the analysis of XRR and electrical data of as-deposited and annealed (in N_2 ambient for 1 hour) hydrogenated amorphous silicon nitride films deposited on Si substrate under different conditions. The roughness indicated in the table corresponds to the top surface of the individual layer *i.e.* (top, middle and interfacial layer). The estimated error in the values of D_{it} is ±10%.

Sample	Condition	Thickness (nm), Density (g/cm^3), Roughness (nm)			V_{fb} (V)	D_{it} ($\times10^{12}$)
		Top layer	Middle layer	Interfacial layer		(cm^{2}eV^{-1})
$R=0.02$	ASD	7.5, 1.8, 2.2	87.2, 1.9, 1.2	2.0, 1.6, 0.2	13.6	3.43
	900 °C	5.5, 1.7, 3.0	70.2, 2.5, 1.7	1.8, 2.2, 0.2	12.4	2.58
	1000 °C	5.5, 1.7, 3.8	70.9, 2.5, 1.6	2.6, 2.3, 0.3	10.2	2.51
	1100 °C	3.6, 1.7, 3.0	72.0, 2.4, 0.9	3.0, 2.4, 0.3	12.5	1.11
$R=0.04$	ASD	2.4, 1.8, 0.6	85.7, 1.9, 0.8	2.0, 2.0, 0.3	9.5	1.42
	900 °C	2.0, 2.2, 0.8	64.1, 2.4, 0.8	1.8, 2.4, 0.3	13.1	3.70
	1000 °C	2.5, 2.5, 1.1	61.9, 2.7, 1.5	2.5, 2.7, 0.3	12.4	4.08
	1100 °C	5.7, 2.2, 1.6	56.7, 2.6, 2.5	3.1, 2.3, 0.3	12.3	1.98

We now turn to the study of individual layers in ASD samples and their evolution on annealing. Considering the middle layer, for ASD $R = 0.02$ and $R = 0.04$ samples the thicknesses of the middle layer (SiN_x) are 87.2 and 85.7 nm, respectively, which basically remains unchanged within the analysis uncertainty of 0.8 nm. This indicates that the effect of the gas flow rate ratio on the growth rate of the a-$SiN_x:H$ layer is negligible within the samples studied, but in order to clarify this point further study of a-$SiN_x:H$ with different "R" values is required. The densities of the same are 1.9 ± 0.1 g/cm^3. However, the aforementioned value of density of the middle layer, labelled as region 2 in fig. 2 is significantly less (~39%) than that of the bulk Si_3N_4 density (3.1 g/cm^3). This is due to hydrogen incorporated void structure during deposition. A detailed H content analysis by elastic recoil detection analysis (ERDA) of the films grown under similar conditions supports this fact and has been reported elsewhere [18]. The roughness of the middle layer is 1.2 ± 0.06 nm for $R=0.02$ as compared to 0.8 ± 0.04 nm for the $R=0.04$ sample, which clearly suggests a denser structure (*i.e.* dominant SiN_x) in the ASD $R=0.04$ sample. This is in accordance with the X-ray photoelectron spectra (not shown here) that clearly reveal a predominant silicon nitride phase in the $R=0.04$ sample as compared to the ASD $R=0.02$ sample, which in turn is expected as the flow rate of SiH_4 was increased for the $R=0.04$ sample. In addition, consistent with our earlier studies [18] XPS data reveal the presence of other phases such as silicon oxynitride (SiO_xN_y) and SiO_2 were also detected, and justify the presumption of taking the top layer as a mixture of SiO_2 and SiN_x in the XRR fitting.

The topmost layer (labelled as region 1 in fig. 2) has density 1.8 ± 0.1 g/cm^3, thickness 7.5 ± 0.07 and 2.4 ± 0.02 nm of ASD $R = 0.02$ and $R = 0.04$ samples, respectively. As stated earlier, the origin of this top layer is due to oxidation of the surface of the samples on exposure to ambient air. In spite of the fact that samples were kept under similar conditions after deposition, the difference in the thickness of the top layer implies that the oxidation of the ASD samples surface does not proceed at the same rate. The oxidation rate is higher in the ASD $R=0.02$ sample as compared to the $R=0.04$ one. Banerjee *et al.* have reported that in particular, the silicon nitride having high density will promote dense oxidation at a slower rate [19]. Therefore, we attribute the difference in the thickness of the top layer to the lower oxidation rate of silicon nitride, as the presence of the dominant silicon nitride phase in the ASD $R=0.04$ sample as compared to the $R=0.02$ one, is revealed by our XPS results. This is further supported by the low roughness of the top layer for the ASD $R=0.04$ sample as compared to the $R=0.02$ one (see table 1).

In addition to the above, more interestingly we observe the formation of a 2.0 ± 0.02 nm thick IL (labelled as region 3 in fig. 3) between SiN_x and Si in both the ASD $R = 0.02$ and $R = 0.04$ samples. This IL is inherently formed during the initial stage of the growth process. Further, it can be noticed that the density of the IL between SiN_x and Si depends upon the growth conditions, as it is 1.6 ± 0.1 and 2.0 ± 0.1 g/cm^3 for $R=0.02$ and 0.04 samples, respectively (see table 1). The disparity in the density of the IL in the ASD samples is due to the presence of extrinsic Si dangling bonds with different back bond configurations having atoms such as Si, N, H and O during the initial stages of film growth. The presence of oxygen is due to the uncontrollable oxidation layer formed while loading the sample and the residual oxygen present in the photo-CVD chamber. Therefore, the IL is also considered as a mixture of SiO_2 and a-$SiN_x:H$. The roughnesses of the IL for the ASD $R=0.02$ and $R=0.04$ samples are 0.2 ± 0.01 nm and 0.3 ± 0.01 nm, respectively. The increase in roughness as "R" is increased results from the decrease in energy (and therefore surface mobility) of the high molecular species arriving on the surface. The formation of high molecular species with the increase in the flow rate of silane during the deposition of a-$SiN_x:H$ films in the photo-CVD chamber is well known [20].

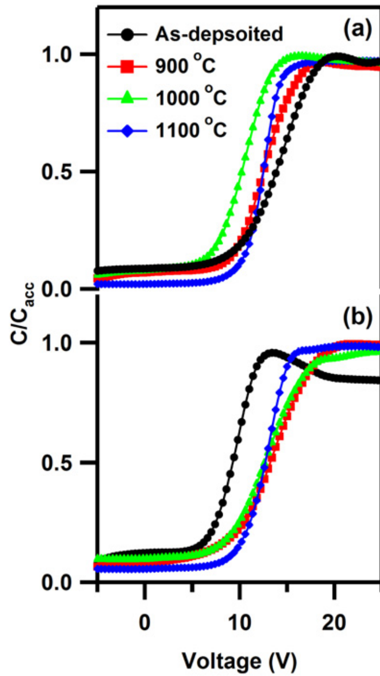

Fig. 3: (Colour on-line) High-frequency (1 MHz) C-V characteristic of the as-deposited and annealed samples at different temperatures for sample (a) $R=0.02$ and (b) $R=0.04$, respectively.

It is generally predicted that the annealing is associated with interatomic rearrangements towards more in equilibrium bonding arrangement characterized by the dense/crystalline structure. The ASD a-$SiN_x:H$ films generally have an amorphous network which is metastable as compared to stoichiometric Si_3N_4 as it contains H. Therefore annealing causes out-diffusion of hydrogen attributed to breaking of Si-H and N-H bonds, hence Si–N–Si cross-linking, which leads to the formation of a denser structure. This densification is experimentally evidenced in our XRR results (see fig. 1 and table 1) as the overall compaction on an average is 18.9% and 25.9% (taking the total thickness into account) for the sample $R=0.02$ and $R=0.04$, respectively. On increasing the annealing temperature (T_a), the thickness and density of the middle layer of the ASD $R=0.02$ sample almost remain constant, whereas the ASD $R=0.04$ sample exhibits a significant decrease in thickness and increase in density up to a maximum of $2.7\,g/cm^3$ (*i.e.* 87% of bulk Si_3N_4 density), within the uncertainty of 0.7 nm and $0.1\,g/cm^3$, respectively (see table 1). It is reasonable to conclude that the sample with lower "R" value shows resistance towards annealing. This behaviour is similar to that observed by Cai *et al.* during the rapid thermal annealing of plasma-enhanced chemical vapor-deposited (PECVD) silicon nitride films with higher refractive indices (*i.e.* higher "R" values) [21] but it was not explained. We believe that since SiN_4 tetrahedra are similar to SiO_4, the structural relaxation of the a-$SiN_x:H$ films on annealing due to out-diffusion of hydrogen in the $R=0.04$ sample is governed by the mutual reorientation of the SiN_4 tetrahedra rather than by the free volume, which could be the case for $R=0.02$ samples. Rendell *et al.* have already demonstrated an anomalous structural relaxation in SiO_2 films [22].

In addition to this, for samples annealed at 900 °C, a decrease in thickness of the top layer is observed within an uncertainty of 0.8 nm for the $R=0.02$ sample and of 0.02 nm for the $R=0.04$ one; see table 1. Further increasing T_a does change the thickness of the top layer appreciably for the $R=0.02$ sample but an increase in thickness is noticed in the case of the $R=0.04$ sample (see table 1). Apart from this, the density of the top layer remains constant at a value of $1.7\pm0.1\,g/cm^3$ in the case of $R=0.02$, whereas it increases up to $2.5\pm0.1\,g/cm^3$ for the $R=0.04$ sample annealed at 1000 °C. The increase in the density of the top layer is due to the formation of the silicon oxynitride phase on annealing at high temperature. The formation of a high-density silicon oxynitride layer on the top of the silicon nitride film on annealing in N_2 ambient has been established recently [23]. Now we address the anomalous behaviour shown by the $R=0.04$ sample in terms of density and thickness on annealing at 1000 and 1100 °C, respectively. Schmidt *et al.* [24] have shown that amorphous silicon nitride on isothermal annealing undergoes a structural relaxation, which has significant influence on the nitrogen diffusion. In view of this from, table 1 it is apparent that for the ASD $R=0.04$ sample annealed at 1000 °C the density of all the layers is almost near to that of silicon nitride, which implies an unrelaxed structure [25]. Therefore, when the ASD $R=0.04$ sample is annealed at 1100 °C it undergoes a relaxation process that is evidenced by the decrease in density of the individual layers with changes in their thickness.

From table 1 and region 3 of the EDP profile (fig. 2), as expected, there is an increase in density and decrease in thickness of the IL between SiN_x and Si on annealing at 900 °C. More interesting to note is that on further increasing T_a, an increase in the thickness of the IL is observed for both the ASD $R=0.02$ and the $R=0.04$ sample from 2.0 to 3.0 ± 0.03 nm and from 2.0 to 3.1 ± 0.03 nm, respectively. It should be pointed out here that this change in thickness directed along the surface normal could be detected by XRR, as it measures the in-plane electron density averaged over the coherence length of the X-ray beam. Furthermore, for the ASD $R=0.02$ sample the density of the IL varies in the range 2.2–$2.4\pm0.1\,g/cm^3$ which is almost constant and that of the ASD $R=0.04$ sample increases from $2.0\pm0.1\,g/cm^3$ up to a maximum of $2.7\pm0.1\,g/cm^3$ and then decreases down to $2.3\pm0.1\,g/cm^3$. Since the density of Si_3N_4 ($3.1\,g/cm^3$) is higher than that of Si ($2.33\,g/cm^3$) and SiO_2 ($2.20\,g/cm^3$), the increase in the width and density of IL for the $R=0.02$ and 0.04 samples is attributed to the structural relaxation and/or substantial elemental diffusion on annealing across the interface and throughout the film. This is consistent

with the reports on other dielectrics as well as for silicon nitride [26–28].

In order to check whether this difference in morphology and density has any influence on the electrical properties of these thin films, *C-V* measurements were carried out. High-frequency *C-V* curves for all the samples are shown in fig. 3. The interface-state density ($D_{\rm it}$) and flat-band voltage ($V_{\rm fb}$) as calculated from the 1 MHz *C-V* characteristics using Terman's method [29] are listed in table 1. A large positive shift in the $V_{\rm fb}$ indicates the presence of a significant amount of negative charges in the ASD and annealed samples. Park *et al.* [30] have also reported the presence of negative charges in low-temperature deposited SiN_x. As proposed by Park *et al.* [30], we also expect the presence of negative charges in ASD samples to depend upon the different ratio of N-H/Si-H bonds. As the flow rate of silane is increased the probability of the Si-H bond and SiN_x phase formation increases, hence the observed negative shift in $V_{\rm fb}$ (see fig. 3). $R = 0.02$ annealed samples initially exhibit negative shift in $V_{\rm fb}$ then a positive shift which suggests generation of both positive and negative charges. In contrast, sample $R = 0.04$ exhibits a positive shift in $V_{\rm fb}$ on annealing at 900 °C and then a reverse shift on further increasing $T_{\rm a}$. However in this case it seems that there is no appreciable creation of positive charges and the dominant fixed charges are negative, which are normally generated due to annealing in N_2 ambient [31]. Based on the aforementioned experimental observations, it is clear that even though the annealing conditions are the same, the $V_{\rm fb}$ shifts are different for different growth conditions, resulting from the creation of positive and negative charges in the film or at the interface on annealing.

The two samples ($R = 0.02$ and 0.04) show different behaviour in terms of $D_{\rm it}$. This can only be understood in the terms of the IL density. In the ASD $R = 0.04$ sample $D_{\rm it}$ is less as compared to that of the $R = 0.02$ sample. One can interpret this in terms of the density of the IL, as for $R = 0.04$ it is $2.0 \pm 0.1\,{\rm g/cm^3}$ nearly that of SiO_2 ($2.20\,{\rm g/cm^3}$) which is known to exhibit excellent interface integrity with Si. On the other hand as revealed by the increase in density of the IL on annealing, this decrease in $D_{\rm it}$ for the $R = 0.02$ sample is due to a greater incorporation of nitrogen in the IL, that leads to a random bonding configuration phase of SiO_xN_y sandwiched between the SiN_x film and the Si substrate. The presence of positive charges in the SiO_xN_y IL [32,33] and the low interface trap density associated with it is well documented [34]. In contrast, for $R = 0.04$ the increase in density of the IL approaches a value which is $\sim 85\%$ that of bulk Si_3N_4 (see table 1). It is reported that the introduction of Si-N bonds near the Si surface leads to increased rigidity [35] and in order to release this stress more dangling bonds are created [36], consequently $D_{\rm it}$ increases. Theoretically Lucovsky *et al.* have also anticipated on the basis of bonding constraint model that Si–Si_3N_4 interfaces do not display excellent interface properties [37]. A drastic decrease in the $D_{\rm it}$ for the $R = 0.04$ sample annealed at 1100 °C could be correlated with the structural relaxation of Si-N and Si-O bonds into less strained Si-O-N bonds at the interface, causing a decrease in the IL density with a corresponding increase in the layer thickness as seen in table 1. This structural relaxation caused by annihilation of defects is very likely to be the same as observed in amorphous silicon nitride [24].

In summary, the present study clearly reveals that the density and roughness of the ultra-thin interface layer at the SiN_x/Si interface is markedly different for different growth conditions. The variation in the density of the interfacial layer as revealed by XRR is interpreted in terms of anneal-induced structural relaxation. As a consequence, interface state density ($D_{\rm it}$), which could be due to incorporation/self-diffusion of nitrogen and its thermal instability gets modified. However, further investigations are required to quantitatively understand the presence of negative charges in the as-deposited hydrogenated amorphous silicon nitride thin films for future electrical applications.

* * *

The authors would like to thank Dr G. S. Lodha from the X-ray Optics Section, RR-CAT, Indore, India for fruitful discussions. The authors appreciate the technical help of Mr M. Chandrasekhar. One of the authors (SPS) gratefully acknowledges the Indian Institute of Technology Delhi for financial support.

REFERENCES

[1] Carcia P. F., Mclean R. S., Reilly M. H., Crawford M. K., Blanchard E. N., Kattamis A. Z. and Wagner S., *J. Appl. Phys.*, **102** (2007) 074512.

[2] Tiwari S. P., Srinivas P., Shriram S., Kale N. S., Mhaisalkar S. G. and Rao V. R., *Thin Solid Films*, **516** (2008) 770.

[3] Flora M. Li, Nathan A., Yiliang Wu and Beng S. Ong., *Appl. Phys. Lett.*, **90** (2007) 133514.

[4] Remashan V., Jang J. H., Hwang D. K. and Park S. J., *Appl. Phys. Lett.*, **91** (2007) 182101.

[5] Wu Y., Liu P., Ong B. S., Srikumar T., Zhao N., Botton G. and Zhu S., *Appl. Phys. Lett.*, **86** (2005) 141102.

[6] Liu P., Wu Y., Li Y., Ong B. S. and Zhu S., *J. Am. Chem. Soc.*, **128** (2006) 4554.

[7] Houssa M., Naili M., Zhao C., Bender H., Heyns M. M. and Stesmans A., *Semicond. Sci. Technol.*, **16** (2001) 31.

[8] Copel M., Gribelyuk M. and Gusev E., *Appl. Phys. Lett.*, **76** (2000) 436.

[9] Green M. L., Gusev E. P., Degraeve R. and Garfunkel E. L., *J. Appl. Phys.*, **90** (2001) 2057.

[10] Aratani T., Higuchi M., Sugawa S., Ikenaga E., Ushio V., Nohira H., Suwa T., Teramoto A., Ohmi T. and Hattori T., *Appl. Phys. Lett.*, **104** (2008) 114112.

[11] Martínez F. L., Prado Del A., Mártil I., González-Díaz G., Kliefoth K. and Füssel W., *Semicond. Sci. Technol.*, **16** (2001) 534.

[12] Bauer E., Wei Y., Mueller T., Pavlovska V. and Tsong I. S. T., *Phys. Rev. B*, **51** (1995) 17891.

[13] Schmidt Th., Clausen T., Brumke O., Gangodadhyay S., Falta J., Flege J. I., Heun S., Bernsdorf S., Gregoratti L. and Kiskinova M., *Nucl. Instrum. Methods, Phys. Res. B.*, **200** (2003) 79.

[14] Kim J. E. and Yeom H. W., *Phys. Rev. B*, **67** (2003) 035304.

[15] Rai S., Tiwari M. K., Lodha G. S., Modi M. H., Chattopadhyay M. K., Majumdar S., Gardelis S., Viskadourakis Z., Giapintzakis J., Nandedkar R. V., Roy S. B. and Chaddah P., *Phys. Rev. B*, **73** (2006) 035417.

[16] Chason E. and Mayer T. M., *Crit. Rev. Solid State Mater. Sci.*, **22** (1997) 1.

[17] Parratt L. G., *Phys. Rev.*, **95** (1954) 359.

[18] Singh S. P., Srivastava P., Ghosh S., Khan S. A. and Prakash G. Vijaya., *J. Phys.: Condens. Matter*, **21** (2009) 095010.

[19] Banerjee S., Ferrari S., Piagge R. and Spandoni S., *Appl. Phys., Lett.*, **84** (2004) 3798.

[20] Rathi V. K., Gupta M., Thangaraj R., Chari K. S. and Agnihotri O. P., *Thin Solid Films*, **266** (1995) 219.

[21] Cai L., Rohatgi A., Yang D. and El-Sayed M. A., *J. Appl. Phys.*, **80** (1996) 5384.

[22] Rendell R. W. and Nagi K. L., *Appl. Phys. Lett.*, **57** (1990) 2428.

[23] Liu Z., Ito S., Wilde M., Fukutani K. and Koganezawa T., *Appl. Phys. Lett.*, **92** (2008) 192115.

[24] Schmidt H., Gruber W., Gutberlet T., Ay M., Stahn Nj., Geckle U. and Bruns M., *J. Appl. Phys.*, **102** (2007) 043516.

[25] Jung Y. G., Pajares A. and Lawna B. R., *J. Mater. Res.*, **19** (2004) 3569.

[26] Ramani K., Essary C. R., Son S. Y., Craciun V. and Singh R. K., *Appl. Phys. Lett.*, **89** (2006) 242902.

[27] Lu Z. H., Tray S. P., Rao R. and Pianetta P., *Appl. Phys. Lett.*, **67** (1995) 2836.

[28] Schmidt H., Gupta M. and Bruns M., *Phys. Rev. Lett.*, **96** (2006) 055901.

[29] Terman L. M., *Solid-State Electron.*, **5** (1962) 285.

[30] Park K. J. and Parsons G. N., *J. Vac. Sci. Technol. A*, **22** (2004) 2256.

[31] Hakvoort R. A., Schut H., Veen A. Van, Arnold Bik W. M. and Habraken F. H. P. M., *Appl. Phys. Lett.*, **59** (1991) 1687.

[32] Aberle A. G., *Crystalline Silicon Solar Cells: Advanced Surface Passivation And Analyses* (University of New South Wales, Centre for Photovoltaic Engineering, Sydney) 1999.

[33] Schmidt J. and Aberle A. G., *J. Appl. Phys.*, **85** (1999) 3626.

[34] Poon M. C., Kok C. W., Wong H. and Chan P. J., *Thin Solid Films*, **462** (2004) 42.

[35] Stesmans A. and Van Gorp G., *Phys. Rev. B*, **52** (1995) 8904.

[36] Stesmans A., *Phys. Rev. B*, **48** (1993) 2418.

[37] Lucovsky G., Wu Y., Niimi H., Misra V. and Phillips J. C., *Appl. Phys. Lett.*, **74** (1999) 2005.